THE UNIVERSITY of EDINBURGH

Edinburgh Research Explorer

Verbal working memory and functional large-scale networks in schizophrenia

OPEN ACCESS
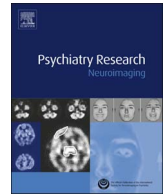
Verbal working memory and functional large-scale networks in schizophrenia

Maria R. Dauvermann[a,b,c,*], Thomas WJ Moorhead[a], Andrew R. Watson[a], Barbara Duff[a], Liana Romaniuk[a], Jeremy Hall[a,d], Neil Roberts[e,f], Graham L. Lee[c], Zoë A. Hughes[g], Nicholas J. Brandon[g,h], Brandon Whitcher[i], Douglas HR Blackwood[a], Andrew M. McIntosh[a], Stephen M. Lawrie[a]

[a] Division of Psychiatry, Royal Edinburgh Hospital, Morningside Park, University of Edinburgh, Edinburgh EH10 5HF, UK
[b] School of Psychology, National University of Ireland Galway, University Road, Galway, Ireland
[c] McGovern Institute for Brain Research, Massachusetts Institute of Technology, 43 Vassar Street, Cambridge, MA 02139, USA
[d] Neuroscience and Mental Health Research Institute, Cardiff University, Cardiff, UK
[e] Clinical Research Imaging Centre, University of Edinburgh, Edinburgh, UK
[f] British Heart Foundation Centre for Cardiovascular Science, University of Edinburgh, Edinburgh, UK
[g] Neuroscience Research Unit, Pfizer Inc., Cambridge, MA, USA
[h] IMED Neuroscience Unit, AstraZeneca, Waltham, MA, USA
[i] Clinical and Translational Imaging, Pfizer Inc., Cambridge, MA, USA

ARTICLE INFO

ABSTRACT

The aim of this study was to test whether bilinear and nonlinear effective connectivity (EC) measures of working memory fMRI data can differentiate between patients with schizophrenia (SZ) and healthy controls (HC). We applied bilinear and nonlinear Dynamic Causal Modeling (DCM) for the analysis of verbal working memory in 16 SZ and 21 HC. The connection strengths with nonlinear modulation between the dorsolateral prefrontal cortex (DLPFC) and the ventral tegmental area/substantia nigra (VTA/SN) were evaluated. We used Bayesian Model Selection at the group and family levels to compare the optimal bilinear and nonlinear models. Bayesian Model Averaging was used to assess the connection strengths with nonlinear modulation. The DCM analyses revealed that SZ and HC used different bilinear networks despite comparable behavioral performance. In addition, the connection strengths with nonlinear modulation between the DLPFC and the VTA/SN area showed differences between SZ and HC. The adoption of different functional networks in SZ and HC indicated neurobiological alterations underlying working memory performance, including different connection strengths with nonlinear modulation between the DLPFC and the VTA/SN area. These novel findings may increase our understanding of connectivity in working memory in schizophrenia.

1. Introduction

Schizophrenia is a severely disabling illness that is characterized by positive and negative symptoms as well as cognitive deficits. It is thought that such cognitive deficits are often associated with working memory deficits (Bozikas and Andreou, 2011; Genevsky et al., 2010; Gold, 2004). Evidence comes from functional Magnetic Resonance Imaging (fMRI)[1] studies including functional connectivity (FC) and effective connectivity (EC) studies in verbal working memory in patients with schizophrenia (SZ) and healthy controls (HC). Such studies repeatedly reported cortical dysconnectivity in SZ when compared to HC (Birnbaum and Weinberger, 2013; Dauvermann et al., 2014; Deserno et al., 2012; Glahn et al., 2005; Schlosser et al., 2003a, 2003b, 2006; Schmidt et al., 2013, 2014).

Evidence from animal studies proposes that activity-dependent synaptic plasticity processes (Abbott et al., 1997; Rothman et al., 2009)

---

are modulated via nonlinear effects. These nonlinear and glutamatergic modulation processes encompass the meso-cortical and cortico-mesal connections (Pan and Zucker, 2009; Salinas and Sejnowski, 2001; Wang, 2010) and are implicated in working memory (Berends et al., 2005; Durstewitz and Seamans, 2002, 2008; Gao et al., 2003; Laruelle et al., 2005; Murphy and Miller, 2003; Neher and Sakaba, 2008; Pan and Zucker, 2009; Salinas and Sejnowski, 2000; Sun and Beierlein, 2011; Tseng and O'Donnell, 2004; Tzschentke, 2001; Volman et al., 2010), which also involve dopaminergic modulation processes (Coyle, 2006; Javitt, 2007; Tanaka, 2006). For human neuroimaging studies, it has been shown that the connection from the ventral tegmental area/ substantia nigra (VTA/SN) area to the dorsolateral prefrontal cortex (DLPFC) (i.e. the meso-cortical connection) is implicated in working memory function (D'Ardenne et al., 2012; Murty et al., 2011). Furthermore, for SZ it has been proposed that blood oxygen level-dependent (BOLD) responses during working memory in SZ could be explained by underlying gating mechanisms of the meso-cortical connection when compared to HC (Braver et al., 1999; Braver and Cohen, 1999). In other words, observed changes in BOLD responses and cortical connectivity may be driven by altered connection strengths with nonlinear modulation of the meso-cortical and/or cortico-mesal connections.

The Dysconnection Hypothesis posits that the *N*-Methyl-D-aspartate receptor (NMDA-R) hypofunction model for schizophrenia could be underlying the pathophysiological pathways of altered synaptic plasticity processes and thus result in cortical dysconnectivity in schizophrenia (Friston et al., 2016; Friston and Frith, 1995; Stephan et al., 2006, 2009; Weinberger, 1993). In clinical studies, the non-invasive and indirect investigation of the NMDA-R hypofunction model can be modeled by Dynamic Causal Modeling (DCM) for fMRI. DCM is a biophysical modeling approach of neuronal dynamic processes (Friston and Dolan, 2010; Friston et al., 2003) that integrates functional large-scale models with Bayesian inversion methods (Daunizeau et al., 2011a; Friston and Dolan, 2010). DCM evaluates inter-regional EC through assessment of experimental modulation of a given experimental task (Friston et al., 2003) within *a priori* defined functional large-scale networks. Nonlinear DCM, an extension of bilinear DCM, allows for the inference about nonlinearities in fMRI data (Stephan et al., 2008).

We hypothesized that the connection strengths with nonlinear modulation from the VTA/SN area to the DLPFC would be altered in contrast to the connection strength with nonlinear modulation from the DLPFC to the VTA/SN as a potential measure of working memory disruption between SZ and HC. To test this hypothesis, we applied bilinear and nonlinear DCM for fMRI in separate analysis steps to investigate functional large-scale networks in the verbal "N-Back" task in SZ and HC.

2. Methods

2.1. Subjects

Sixteen SZ and 21 HC participated in the verbal working memory fMRI task. SZ and HC were recruited from the Royal Edinburgh Hospital, associated hospitals and the Scottish Mental Health Research Register (http://www.smhrn.org.uk/). Diagnosis of schizophrenia was based on interview using the Structured Clinical Interview for DSM-IV (First et al., 2002). SZ were also assessed with the Positive and Negative Syndrome Scale (Kay et al., 1987), Scale for the Assessment of Negative Symptoms (Andreasen, 1989) and the Global Assessment of Function (Pedersen and Karterud, 2012). Inclusion criteria included (i) diagnosis of established schizophrenia as assessed, and (ii) no acute psychotic symptoms at the time of the scan. Exclusion criteria included (i) history of any major psychiatric illness other than schizophrenia, (ii) history of severe brain injury, (iii) history of a neurological disorder, and (iv) dependency or harmful use of alcohol or drugs during the last 12 months. Also, HC were excluded if they had a family history of

schizophrenia. All participants provided written informed consent. The study was approved by the local Research Ethics Committee.

2.2. Functional experimental details

All participants performed the verbal "2-Back" task known to show a consistent functional large-scale network of BOLD responses (Owen et al., 2005). They were presented with a sequence of single capital letters (Broome et al., 2009). The experimental block design consisted of (i) the baseline or "0-Back" condition; (ii) the "1-Back" condition; and (iii) the "2-Back" condition. Behavioral task performance was analyzed with the sensitivity index *d'* (Eq. (1)) (Macmillan and Creelman, 1991).

$$d' = z(Hits) - z(Falsealarm \quad s)$$
$$z = \text{statistical } Z \text{ value} \tag{1}$$

Hits and false alarm rates were adjusted as previously reported (Macmillan and Kaplan, 1985). For the fMRI and DCM analyses, SZ and HC were selected based on comparable good behavioral performance level in the "N-Back" task to control for behavioral performance impairments on BOLD response (Eryilmaz et al., 2016) and EC measures. Briefly, the cut-off for good behavioral performance was set at *d'* > 1.93 which equals a hit rate > 85% and false alarm rate < 20% across all participants. *D'* values were entered in a general linear model with group as fixed factor and age and gender as covariates.

2.3. Functional scanning procedure

Brain imaging was carried out at the Clinical Research Imaging Centre at the Queen's Medical Research Institute (Edinburgh, UK) on a Siemens 3 T whole-body MRI Verio scanner (Siemens Medical Systems, Erlangen, Germany) using the matrix head coil with 12 elements. Structural scans, verbal "N-Back" EPI scans were acquired during the same scanning session in all participants.

An initial localizer scan was performed to measure the inter-hemispheric angle and the AC-PC line. The structural images were acquired using T_1-weighted, magnetization prepared rapid acquisition gradient echo images prescribed parallel to the AC-PC line, providing 160 sagittal slices of 1 mm thickness, 256×256 mm^2 FOV, matrix size 256×256 mm^2. Further scan parameters were TR = 2300 ms, TE = 2.98 ms, TI = 900 ms and flip angle = 9°. EPI scans for the "N-Back" task were acquired continuously during the experimental task (TR/TE = 1560/ 26 ms, matrix size of 256×256 mm^2; FOV 256×256 mm^2). Twenty six interleaved slices with 4 mm slice thickness were acquired. Each EPI sequence encompassed 293 volumes of which the first six volumes were discarded.

2.4. FMRI data analysis

FMRI data processing and statistical analyses were performed in SPM8 (http://www.fil.ion.ucl.ac.uk/spm/) running in Matlab (version 7.1; The MathWorks, Natick, MA, USA). All functional volumes were spatially realigned, normalized to MNI space and spatially smoothed with an isotropic 8 mm full-width at half-maximum Gaussian kernel.

For the statistical analyses, the onset times for each condition were convolved using a canonical hemodynamic response function. For the design matrix, the temporal reference has been set to the middle slice in the EPI acquisition where the TR was set to 1560 ms. The main contrast of interest was defined as "0-Back" < "2-Back" with age and gender as covariates. From this second-level analysis, we generated statistical parametric maps of the *T* statistic and *F* statistic at each voxel SPM (Constantinidis and Klingberg, 2016), which denoted differences in activation for the main contrast of interest. The statistical parametric maps were thresholded at *p* < 0.001 uncorrected. Regions are reported that survived cluster-level correction for multiple comparisons across

the whole brain at $p < 0.05$. For the ACC and the VTA/SN area, we applied a threshold of $p < 0.05$ FDR in accordance with a previous report (Genovese et al., 2002).

2.4.1. Dynamic Causal Modeling

DCM analyses were run using DCM8 (revision number 3684) as implemented in SPM8 to assess EC in the verbal "N-Back" task. Bilinear and nonlinear DCM was run following the heuristic search protocol (Dauvermann et al., 2013). The connections strengths modeled for the bilinear models and nonlinear models followed the original equations (Friston et al., 2003; Stephan et al., 2008; Penny et al., 2010): Matrix A denotes the endogenous connection strength in the absence of experimental manipulations; matrix B resembles the modulation of those endogenous connections by the experimental manipulation induced by the main contrast of interest; matrix C reflects driving inputs, which represent extrinsic parameters that change the neuronal state of brain regions within the model; and matrix D denotes the gating of a connection between two regions by the activity of a third region.

2.4.1.1. Region of interest selection and time series extraction. The selection of the regions of interest (ROIs) was based on (i) the second-level SPM results of the "0-Back" < "2-Back" contrast, and (ii) reported findings in the literature. Clinical fMRI and PET studies repeatedly reported the involvement of the DLPFC, intra-parietal sulcus (IPS), anterior cingulate cortex (ACC) in terms of FA, FC and task-dependent EC measures during the verbal/numeric "N-Back" task in patients with established schizophrenia (EST) and HC FA, (Callicott et al., 2000, 2003; Carter et al., 1998; Perlstein et al., 2001; Thermenos et al., 2005); FC, (Meyer-Lindenberg et al., 2001, 2005b; Quide et al., 2013; Rasetti et al., 2011; Tan et al., 2006); EC, (Deserno et al., 2012; Schmidt et al., 2013, 2014; Zhang et al., 2013). The VTA/SN area was included in the networks in addition to the established regions of the DLPFC, IPS and ACC to model the functional role of the VTA/SN area in working memory as reported in recent fMRI and PET studies in HC (D'Ardenne et al., 2012; Murty et al., 2011; Xu et al., 2013; Yu et al., 2013) and EST (D'Aiuto et al., 2015). The coordinates of the VTA/SN area are in keeping with these studies on the VTA/SN area in working memory.

Regional time series of the four regions were extracted from the individual's activation map of the contrast thresholded at $P < 0.05$ uncorrected at the closest maxima within a standard distance of 8 mm of the group peak level for the IPS and DLPFC and adjusted distance of 6 mm of the group peak level for the ACC and the VTA/SN area according to previous studies. This procedure ensured that the selected ROIs for the DCM networks were consistent across subjects (Stephan et al., 2007). Participants were selected on the basis of the requirement of activation in all four ROIs in either the left or right hemisphere. This process led to the exclusion of one SZ and three HC. The coordinates of the ROIs are presented in Table 1.

2.4.1.2. Heuristic study protocol. The heuristic search protocol for the

Table 1
Talairach coordinates for the ROIs for the Dynamic Causal Modeling analyses.

Brain regions, BA	Coordinates in Talairach space x, y, z
ACC, BA32	0, 24, 28
Left DLPFC, (BA8; BA9)	−37, 34, 32
Right DLPFC, BA9	37, 42, 27
Left IPS, BA40	−44, −46, 52
Right IPS, BA40	44, −44, 52
Left VTA/SN area	−9, −17, −6
Right VTA/SN area	7, −17, −3

Abbreviations: ACC, anterior cingulate cortex; BA, Brodman areas; DCM, Dynamic Causal Modeling; DLPFC, dorsolateral prefrontal cortex; IPS, intra - parietal sulcus; ROIs, regions of interest; VTA/SN area, ventral tegmental area/substantia nigra area.

application of nonlinear DCM for fMRI (Dauvermann et al., 2013) has been adapted for the verbal "N-Back" task to examine connection strengths with nonlinear modulation of the bidirectional connection between the DLPFC and the VTA/SN area within a network comprising the DLPFC, IPS, ACC and VTA/SN area:

  (i) Phase 1: bilinear DCM
 (ii) Phase 2: nonlinear DCM
(iii) Phase 3: Bayesian Model Averaging (BMA).

In phase 1, bilinear DCM was used in order to select the structure for the working memory network. This analysis contained modulations for the activity-dependent neuronal interactions between the four regions. The optimal model of this analysis was entered into phase 2.

In phase 2, nonlinear DCM was applied to model the connection strengths with activity-dependent modulation of the bidirectional connection between the VTA/SN area and the DLPFC. In order to ensure the modeling of the nonlinear modulation, two preconditions were met: (i) The specification of the nonlinear models was based on the optimal bilinear model from phase 1. Therefore, the bilinear model and the nonlinear models differed only in the single parameter of nonlinearity from each other. (ii) The implementation of Model Space Partitioning and Family Inference was applied to compare between the bilinear and nonlinear models.

In phase 3, the connection strengths with nonlinear modulation in the winning model family were assessed using the posterior densities over connection strengths as assessed with BMA. This step allowed inference of the connection strengths with nonlinear modulation of the bidirectional meso-cortical and cortico-mesal connections.

The three phases of the DCM analyses were run separately for the two groups and both hemispheres.

2.4.1.2.1. Phase 1: Bilinear Dynamic Causal Modeling. The model space of bilinear models consisted of nine functional large-scale networks or DCMs. The DCMs differed in their unidirectional and bidirectional endogenous connections between the four ipsilateral regions of the DLPFC, IPS, ACC and VTA/SN area, whereas the modulations were identical across the nine DCMs (Fig. 1A). Both preclinical and clinical studies of working memory function and gating mechanisms have been used to specify each connection between the regions, each modulation and each input for working memory function to increase the biological interpretability of the biophysical models (Yahata et al., 2017; Dauvermann et al., 2017).

The endogenous connections between the DLPFC, IPS and ACC have been widely modeled based on animal studies that investigated working memory function (Berends et al., 2005; Durstewitz and Seamans, 2002, 2008; Gao et al., 2003; Laruelle et al., 2005; Murphy and Miller, 2003; Neher and Sakaba, 2008; Pan and Zucker, 2009; Salinas and Sejnowski, 2000; Sun and Beierlein, 2011; Tseng and O'Donnell, 2004; Tzschentke, 2001; Volman et al., 2010).

For example, the endogenous connections between the ACC and the VTA/SN area were defined on the basis of known dopaminergic projections (Onn and Wang, 2005). Furthermore, clinical studies were used for the other connections: FC and EC findings for the "N-Back" task were used to specify functional connections between the IPS and the DLPFC (FC, (Quide et al., 2013; Rasetti et al., 2011; Tan et al., 2006); EC, (Deserno et al., 2012; Schmidt et al., 2013, 2014; Zhang et al., 2013), the IPS and ACC (FC, (Meyer-Lindenberg et al., 2001); EC during the Continuous Performance Task (CPT) (Brazdil et al., 2007); the DLPFC and the ACC (Brazdil et al., 2007)). Lastly, the endogenous connections between the DLPFC and VTA/SN area were specified by known dopaminergic projections from the VTA/SN area to the DLPFC (Au-Young et al., 1999; D'Ardenne et al., 2012; Gao and Wolf, 2007; Girault and Greengard, 2004; Takahata and Moghaddam, 1998) and glutamatergic projection from the DLPFC to the VTA/SN area (Tseng and O'Donnell, 2004; Tzschentke, 2001).

Connections with modulatory input were defined by the "0-

a

b
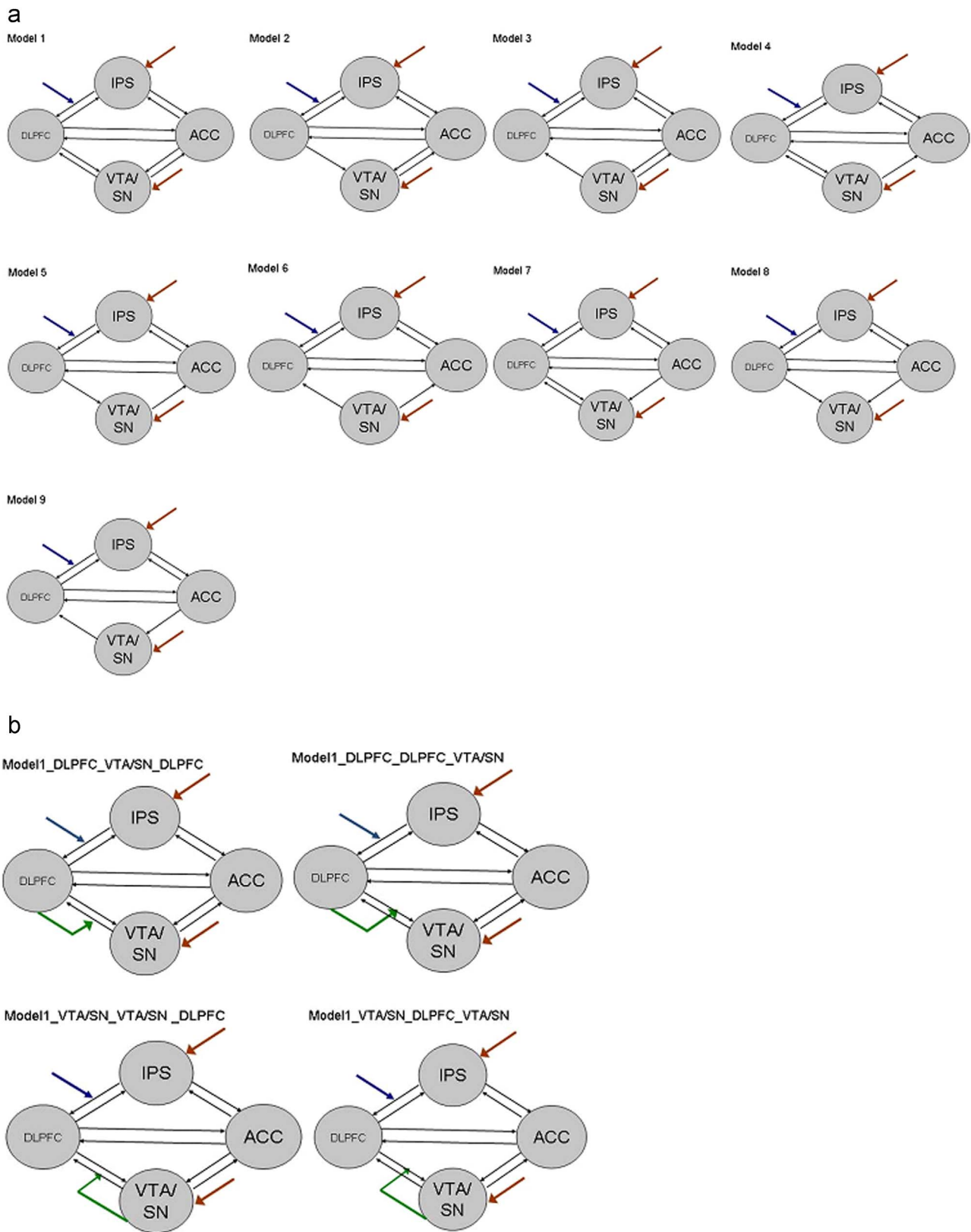
(caption on next page)

Back" < "2-Back" experimental manipulation of the working memory load. Evidence for (parametric) working memory load and interaction effects with working memory load during the "N-Back" task in SZ and HC has been presented for (i) BOLD response results of the bilateral subregions of the prefrontal cortex (PFC) (including the DLPFC), bilateral inferior-parietal lobule (IPL), ACC (Callicott et al., 2000, 2003; Guerrero-Pedraza et al., 2012; Perlstein et al., 2001; Quide et al., 2013; Rasetti et al., 2011; Tan et al., 2006; Thermenos et al., 2005); (ii) FC measures of bilateral subregions of the PFC (including the DLPFC) and bilateral IPL (Quide et al., 2013; Rasetti et al., 2011; Tan et al., 2006)

Fig. 1. Model space of bilinear and nonlinear models. (A) Model space of bilinear models for both groups. All nine models are characterized by bidirectional endogenous connections (black arrow) between the IPS and DLPFC, IPS and ACC and DLPFC and ACC. Furthermore, all models are defined by a modulatory input (blue arrow) on the connection from the IPS to the DLPFC. All models receive two driving inputs (red arrow): One driving input (presented visual stimuli, i.e. single letters) enters the IPS; and one driving input (false alarms) enters the VTA/SN. The nine models differ in the specification of unidirectional or bidirectional endogenous connections: (i) Between the DLPFC and the VTA/SN and (ii) between the ACC and VTA/SN. Model 1 is specified by a bidirectional endogenous connection (i) between DLPFC and VTA/SN and (ii) ACC and VTA/SN. Model 2 is specified by a unidirectional endogenous connection from DLPFC to VTA/SN and a bidirectional endogenous connection between ACC and VTA/SN. Model 3 is specified by a unidirectional endogenous connection from VTA/SN to DLPFC and a bidirectional endogenous connection between ACC and VTA/SN. Model 4 is specified by a bidirectional endogenous connection between DLPFC and VTA/SN and a unidirectional endogenous connection from VTA/SN to ACC. Model 5 is specified by a unidirectional endogenous connection from DLPFC to VTA/SN and a unidirectional endogenous connection from VTA/SN to ACC. Model 6 is specified by a unidirectional endogenous connection from VTA/SN to DLPFC and a unidirectional endogenous connection from VTA/SN to ACC. Model 7 is specified by a bidirectional endogenous connection between DLPFC and VTA/SN and a unidirectional endogenous connection from ACC to VTA/SN. Model 8 is specified by a unidirectional endogenous connection from DLPFC to VTA/SN and a unidirectional endogenous connection from ACC to VTA/SN. Model 9 is specified by a unidirectional endogenous connection from VTA/SN area to DLPFC and a unidirectional endogenous connection from ACC to VTA/SN. (B) Four nonlinear models for patients with schizophrenia. The nonlinear models are specified on the basis of the winning model 1 in SZ. The endogenous connections (black arrow), modulatory input (blue arrow) and driving inputs (red arrow) are defined as in model 1 (Fig. 1A). Model 1_DLPFC_VTA/SN_DLPFC and Model 1_DLPFC_DLPFC_VTA/SN are characterized by the nonlinear modulation (green arrow) from the DLPFC on the bidirectional connection between VTA/SN and DLPFC. Both models are specified upon the winning bilinear model and form model family 2. Model 1_DLPFC_VTA/SN_DLPFC is specified by the nonlinear modulation (green arrow) from DLPFC to the connection from VTA/SN to DLPFC. Model 1_DLPFC _DLPFC_VTA/SN is specified by the nonlinear modulation (green arrow) from DLPFC to the connection from VTA/SN to DLPFC. Model 1_VTA/SN_VTA/SN_DLPFC and model 1_VTA/SN_DLPFC_VTA/SN are characterized by the nonlinear modulation (green arrow) from the VTA/SN on the bidirectional connection between VTA/SN and DLPFC. Both models are specified upon the winning bilinear model and form model family 3. Model 1_VTA/SN_VTA/SN_DLPFC is specified by the nonlinear modulation from VTA/SN to the connection from DLPFC to VTA/SN. Model 1_VTA/SN_DLPFC_VTA/SN is specified by the nonlinear modulation from VTA/SN to the connection from VTA/SN to DLPFC. ACC, anterior cingulate cortex; DLPFC, dorsolateral prefrontal cortex; IPS, intra-parietal sulcus; VTA/SN, ventral tegmental area/substantia nigra.

and (iii) task-dependent EC findings of bilateral subregions of the PFC (including the DLPFC) and bilateral IPL (Deserno et al., 2012; Schmidt et al., 2013, 2014; Zhang et al., 2013).

Driving inputs were defined by previous DCM studies, which reported evidence of effects of visual presentation of stimuli to the IPS (during the CPT), (Brazdil et al., 2007; Wang et al., 2010). The bilinear effects were driven by box car stimulus functions encoding difficulty level of the N-Back task, whereas the driving inputs were driven by box car stimulus functions encoding the main effect of the task.

Bayesian Model Selection (BMS) at the group level has been applied to models of both hemispheres in SZ and HC separately. BMS tests competing hypotheses (the models) about the neural mechanisms generating the data by assessing the model evidence as previously described (Penny et al., 2010, 2004).

2.4.1.2.2. Phase 2: Nonlinear Dynamic Causal Modeling. The objective of modeling the gating mechanism for the bidirectional connection between the DLPFC and the midbrain region comprised of the ventral tegmental area (VTA) and substantia nigra (SN) area during working memory in subjects with schizophrenia and healthy controls, three widely established findings have been incorporated into the models:

- The dopaminergic meso-cortical projection from the VTA/SN area to the DLPFC (bilinear models);
- The glutamatergic projection from the DLPFC to the VTA/SN area (bilinear models); and
- The gain modulation of both of these two connections (nonlinear models).

The model space of nonlinear models comprised four nonlinear networks and was specified on the basis of the optimal bilinear network as outlined in phase 1 of the heuristic search protocol.

The nonlinear modulation of the meso-cortical and cortico-mesal connections is based on evidence from clinical neuroimaging (Braver et al., 1999; Braver and Cohen, 1999) as well as animal and computational studies (Arnsten et al., 2010, 2012; Berends et al., 2005; Tseng and O'Donnell, 2004; Tzschentke, 2001; Wang, 2010).

There were two different optimal models for the "N-Back" task in SZ and HC as a result of the BMS at the group level. Model 1 (bilinear model; Fig. 1A) was the optimal bilinear model for SZ for both hemispheres, whereas as model 7 (bilinear model; Fig. 1A) was the optimal model for HC for both hemispheres.[2] Thus, the nonlinear models were

defined separately for SZ and HC.

For SZ, two nonlinear models were constructed on the structure of the winning Model 1 with nonlinear modulation from the DLPFC to both connections between the DLPFC and the VTA/SN area (i.e. nonlinear models – DLPFC, Fig. 1B). Two further models were defined on the basis of model 1 by the nonlinear modulation from the VTA/SN area to the connections between the DLPFC and the VTA/SN (i.e. nonlinear models – VTA/SN area, Fig. 1B). The nonlinear model space for HC was defined accordingly to model 7.

The previously described BMS inference approach at the model family level, phase 2 of the protocol, has been applied. The BMS analysis was separately run for both groups and both hemisphere. The model space for SZ was partitioned in to three model families:

(i) Model family 1 - optimal bilinear model 1 (Fig. 1A);
(ii) Model family 2 - two nonlinear models with nonlinear modulation from the DLPFC (nonlinear models – DLPFC; Fig. 1B);
(iii) Model family 3 - two nonlinear models with nonlinear modulation from the VTA/SN area (nonlinear models – VTA/SN area; Fig. 1B).

The model space partitioning for HC was defined accordingly to Model 7 and based on the same structure as the model space partitioning for SZ. The Xp for the two winning model families 2 and 3 were summarized as described previously (Dauvermann et al., 2013).

2.4.1.2.3. Phase 3: Connection strength with nonlinear modulation - Bayesian Model Averaging. Bayesian Model Averaging (BMA) has been applied to the winning models from BMS at the model family level as previously applied (Dauvermann et al., 2013), where the posterior densities of the connection strength with nonlinear modulation for the meso-cortical and cortico-mesal connections in the winning models are assessed.

3. Results

3.1. Demographic, clinical and behavioral details

Sixteen SZ and 21 HC underwent the '2-Back' fMRI task of which 15 SZ and 18 HC were included in the DCM analyses (left hemisphere, 13 SZ and 18 HC; right hemisphere, 15 SZ and 16 HC). Full demographic and clinical details including medication details are presented in Table 2. All SZ were treated with antipsychotic medication. Neither task accuracy during the '2-Back' condition nor the response times were

---

[2] In HC, for the right hemisphere model 7 was chosen to enter this phase of the DCM analyses instead of model 8 to enable the modeling of the bidirectional connection

(footnote continued)
between the DLPFC and the VTA/SN area. Exceedance probability (Xp) of model 8 ($Xp = 0.23$) was greater than Xp of model 7 ($Xp = 0.16$) or model 2 ($Xp = 0.18$).

Table 2
Demographic and clinical details.

	Healthy controls	Patients with schizophrenia	Test	p – Value
Number	18	15	–	–
Age	35.00 (14.96)	37.07 (9.95)	$t = -0.457$ ($df = 31$)	$p = 0.651$
Gender (M:F)	13:5	13:2	$x^2 = -0.995$ ($df = 31$)	$p = .327$
IQ (SD)	120.00 (7.81)	107.53 (15.53)	$t = 2.988$ ($df = 31$)	$p = 0.005*$
Handedness (R: L:Mixed)	14:1:2[a]	7:3:2[a]	$x^2 = 3.054$ ($df = 2$)	$p = 0.217$
Level of education (0:1:2)[b]	(3:0:13)[a]	(1:3:11)	$x^2 = 4.139$ ($df = 2$)	$p = 0.120$
Age at illness onset	–	21.47 (6.14)	–	–
Illness duration (in months)	–	93.87 (11.50)	–	–
Total PANSS Score[c]	1.89 (5.16)	21.53 (14.56)	$t = -0.382$ ($df = 31$)	$p < .001*$
Total PANSS Positive Score[c]	0.39 (0.98)	6.00 (4.09)	$t = -0.384$ ($df = 31$)	$p < .001*$
Total PANSS Negative Score[c]	0.11 (0.32)	6.47 (4.94)	$t = -0.418$ ($df = 31$)	$p < .001*$
Total PANSS General Score[c]	1.39 (4.95)	9.20 (8.08)	$t = -0.307$ ($df = 31$)	$p = 0.006$
Total SANS Score	0.78 (2.37)	17.33 (15.09)	$t = -0.4.47$ ($df = 31$)	$p < .001*$
GAF Score	Missing	49.93 (21.52)	–	–
Chlorpromazine equivalent dose[d], Mean (SD)	–	475.00 (400.55)	–	–
Antipsychotic medication[e]	–	(a) 1; (b) 5; (c) 1; (d) 5; (e) 3	–	–
Antipsychotic medication, additional[f]	–	(a) 2; (b) 1	–	–
Other medication[g]	–	(a) 7; (b) 1; (c) 2	–	–

Abbreviations: GAF, Global Assessment of Functioning; PANSS, Positive and Negative Symptom Scale; SANS, Scale for the Assessmentof Negative Symptoms, SD, standard deviation.

[a] Significant at $p < 0.05$ (two-tailed).

[b] 0, Compulsory; 1, More than compulsory; 2, Post-Secondary.

[c] Rescaled total PANSS scores.

[d] To 100 mg CPZ.

[e] Primary medication: (a) Aripiprazole, (b) Clozapine, (c) Depixol (depot), (d) Olanzapine, (e) Risperidone/Risperidone Consta depot.

[f] (a) Amilsulpride, (b) Chlorpromazine.

[g] (a) Antidepressant, (b) Mood Stabilizer, (c) Anticholinergics.

significantly different between HC and SZ.

3.2. Functional MRI results

The main results showed greater activation in the bilateral DLPFC (BA9/46) in HC when compared to SZ (BA9, x = −46, y = 25, z = 31; $P = 0.036$; BA46, x = 41; y = 29, z = 17; $P = 0.044$; Fig. 2A; voxel-wise $P < 0.001$ uncorrected and FWE corrected cluster level). Other regions of greater activation in HC than in SZ included the IPS (BA40) (x = 49, y = −47, z = 30; $P = 0.022$; voxel-wise $p < 0.01$ uncorrected and FWE corrected cluster level), the ACC (BA32) (x = 3, y = 36, z = 26; $P = 0.0243$) and the bilateral midbrain region of the VTA/SN (x = −9, y = −17, z = −6; $P = 0.047$; Fig. 2B; right hemisphere, x = 7, y = −17, z = −3; $p = 0.049$; both at $P < 0.05$ FDR corrected cluster level; Table 3). Briefly, the statistical findings are in keeping with clinical verbal/numeric "N-Back" studies (Callicott et al., 2000; Glahn et al., 2005; Tan et al., 2006; Wang et al., 2010) and the BOLD response of the VTA/SN area had been reported previously in working memory in HC (D'Ardenne et al., 2012; Murty et al., 2011).

3.3. Dynamic Causal Modeling

3.3.1. Phase 1: Bilinear Dynamic Causal Modeling

The exceedance probabilities (Xp) of models 1, 2, 7 and 8 ranged between $Xp = 0.14 - 0.24$ for HC and $Xp = 0.13 - 0.23$ for SZ, respectively. In SZ, model 1 was the optimal model, whereas models 7 and 8 displayed the greater probability in HC.

In SZ, model 1 was the optimal model for both hemispheres (left hemisphere, $Xp = 0.23$; Fig. 3A; right hemisphere, $Xp = 0.20$; Fig. 3B). In contrast, model 7 was the optimal model for the left hemisphere in HC ($Xp = 0.24$; Fig. 3A) whereas model 8 was the optimal model for the right hemisphere ($Xp = 0.23$; Fig. 3B).

Insert Fig. 3

3.3.2. Phase 2: Nonlinear Dynamic Causal Modeling

We report three main results for the BMS analysis at the model family level as described in the model space partitioning:

(i) The nonlinear model families outperformed the bilinear model family in both SZ and HC (left hemisphere, Fig. 4A; right hemisphere, Fig. 4B).

(ii) In SZ, model family 2 was the optimal model family (left hemisphere, $Xp = 0.44$; right hemisphere, $Xp = 0.56$).

(iii) In HC, model family 2 was the winning model family (left hemisphere, $Xp = 0.46$; right hemisphere, $Xp = 0.45$).

It is noted that the results cannot be directly compared between HC and SZ because two different model structures underlie the BMS findings.

3.3.3. Phase 3 - connection strengths with nonlinear modulation

The posterior densities of connection strengths with nonlinear modulation for the meso-cortical and cortico-mesal connections are summarized in Fig. 5. In SZ, the posterior means ranged from −0.02 Hz/0.01 Hz (right/left hemisphere) for the meso-cortical connection to 0.04 Hz (left/right hemisphere) for the cortico-mesal connection. In HC, the posterior means ranged from −0.01 Hz/0.02 Hz (right/left hemisphere) for the meso-cortical connection to 0.001 Hz/0.02 Hz (right/left hemisphere) for the cortico-mesal connection. It is noted that the results cannot be directly compared between HC and SZ because two different model structures underlie the BMS findings.

4. Discussion

This study presents two novel sets of findings on EC measures in functional large-scale networks in working memory in SZ and HC: Firstly, we found that SZ and HC used *different* functional large-scale networks for verbal working memory as measured with bilinear DCM. Secondly, we reported connection strengths with nonlinear modulation in working memory in SZ and HC as inferred by nonlinear DCM.

The main finding of the bilinear DCM analyses revealed that SZ used a *different* bilinear network than HC contrary to the hypothesis of altered connection strengths with nonlinear modulation of the meso-cortical connection of the *same* network. We interpreted the utilization of *different* networks as a potential illness effect since the behavioral performance in the working memory task was comparable between SZ
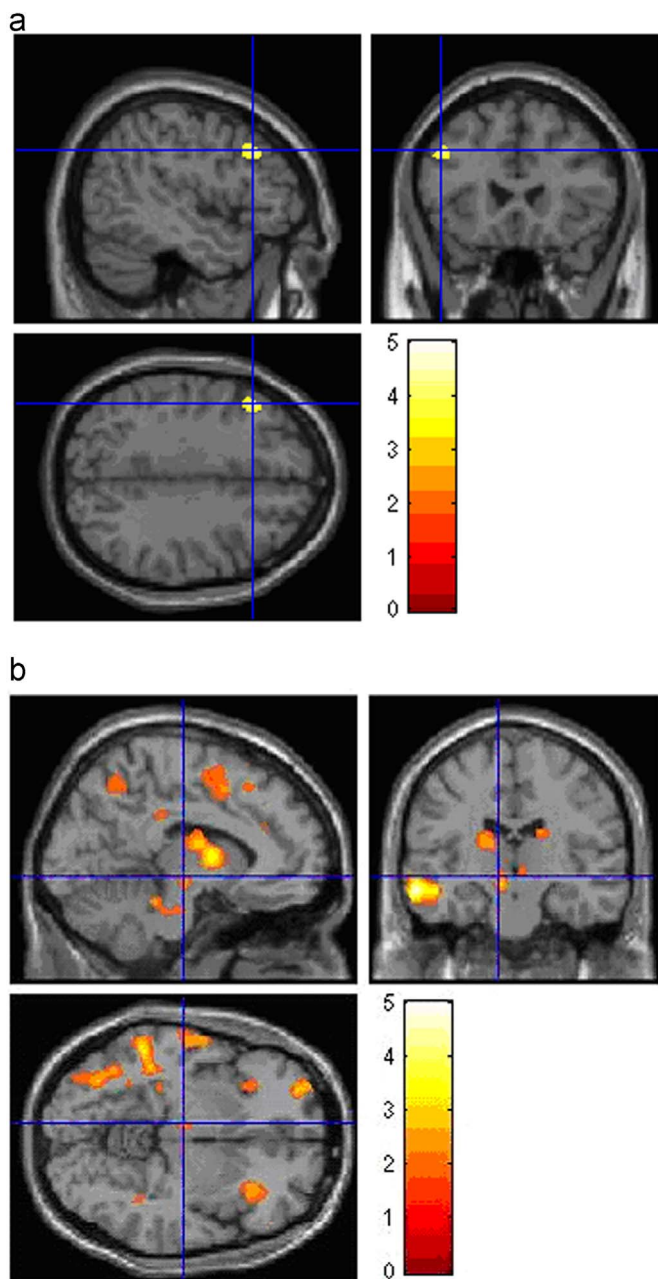
Fig. 2. Between-group results of activation in patients with schizophrenia in contrast to healthy controls. (A) Between-group results - Left MFG, BA9. Reduced activation in patients with schizophrenia in contrast to healthy controls (BA9, x = −46, y = 25, z = 31; P = 0.036). Reported p values are thresholded at voxel-wise p < 0.001 uncorrected and FWE corrected cluster level, extent threshold = 200 voxels. Coordinates represent the three maxima within the same cluster. MFG, middle frontal gyrus. (B) Between-group results - Left Midbrain, VTA/SN. Reduced activation in patients with schizophrenia in contrast to healthy controls (VTA/SN, x = −9, y = −17, z = −6; P = 0.047). Reported p values are thresholded at p < 0.05 FDR corrected cluster level, extent threshold = 200 voxels. Coordinates represent the three maxima within the same cluster. VTA/SN, ventral tegmental area/substantia nigra.

Table 3
Between-group random effects analysis.

P value	Extent	Peak height coordinates	Region	Z score
HC < SZ n/s				
HC > SZ				
0.006[a]	1097	−52, −22, −12 −60, −17, −12	L temporal: middle temporal gyrus, BA21	4.27
0.036[a]	580	−46, 25, 31	L frontal: middle frontal gyrus, BA9	3.83
0.044[a]	345	41, 29, 17	R frontal: middle frontal gyrus, BA46	3.66
0.022[b]	1344	49, −47, 30	R parietal: inferior parietal lobule, BA40	3.56
0.004[c]	1836	−13, −2, 8 −13, −7, 4	L sub-lobar: thalamus	3.50
0.0243[d]	685	3, 36, 26	R limbic: anterior cingulate, BA32	3.53
0.047[d]	267	−9, −17, −6	L midbrain: substantia nigra/ ventral tegmental area	3.32
0.049[d]	204	7, −17, −3	R midbrain: substantia nigra/ ventral tegmental area	3.03

Coordinates represent the three maxima within the same cluster.
Abbreviations: HC, healthy controls; L, left; n/s, not significant; R, right; SZ, individuals with schizophrenia.
[a] Reported P values are thresholded at voxel-wise p < 0.001 uncorrected and FWE corrected cluster level, extent threshold = 200 voxels. Coordinates represent the three maxima within the same cluster.
[b] Reported P values are thresholded at voxel-wise p < 0.01 uncorrected and FWE corrected cluster level, extent threshold = 200 voxels. Coordinates represent the three maxima within the same cluster.
[c] Reported P values are thresholded at p < 0.05 FWE corrected cluster level, extent threshold = 200 voxels. Coordinates represent the three maxima within the same cluster.
[d] Reported P values are thresholded at p < 0.05 FDR corrected cluster level, extent threshold = 200 voxels. Coordinates represent the three maxima within the same cluster.

medication may have affected the task-dependent and nonlinear EC findings. Recent studies showed group differences of task-dependent EC measures of the *same* functional network in the verbal "N-Back" task: (i) Reduced connection strengths with modulatory input of cortico-cortical and cortico-cerebellar connections and increased connection strengths with modulatory input of thalamo-cortical connection in SZ treated with second-generation antipsychotic (SGA) when contrasted to SZ treated with first-generation antipsychotics (FGA) and HC (Schlosser et al., 2003a), and (ii) reduced connection strengths with modulatory input of the prefrontal-parietal connection in patients with first-episode psychosis (FEP) in contrast to HC and subjects at-risk mental state (ARMS) but comparable EC measures with modulatory input between HC and FEP treated with antipsychotic medication (Schmidt et al., 2013). It is not possible to interpret the EC findings of modulatory input and nonlinear modulation in terms of potential pharmacological effects since this study was not designed for such an investigation.[3]

Support for the interpretation of the observed differences in network utilization during the verbal "N-Back" task between SZ and HC comes from three recent DCM studies in SZ (Deserno et al., 2012) and ARMS/FEP that applied bilinear DCM (Schmidt et al., 2013, 2014). In the first study, Deserno et al. (2012) reported reduced task-dependent EC from the DLPFC to the parietal cortex in SZ when compared to HC as assessed with BMA after the observation of *different* optimal networks for SZ and HC (Deserno et al., 2012). Similarly, Schmidt et al. (2013) found progressively reduced task-dependent modulation of EC between the middle frontal gyrus (MFG) and superior parietal lobe (SPL) (from HC to ARMS) when measured with BMA after *different* optimal networks for ARMS, FEP and HC were reported (Schmidt et al., 2013). Lastly, Schmidt et al. (2014) showed decreased task-dependent EC from

and HC. It is also conceivable that the *different* functional large-scale network used by SZ may reflect a compensatory '*network*' mechanism which explains the equally high behavioral performance level compared to HC. This interpretation of findings at the network level extends the widely shared notion that reduced DLPFC BOLD response during working memory in SZ may resemble cortical dysfunction (Schlosser et al., 2008) or a compensation mechanism to impaired cognitive function (Tan et al., 2006). Additionally, it is likely that antipsychotic

---

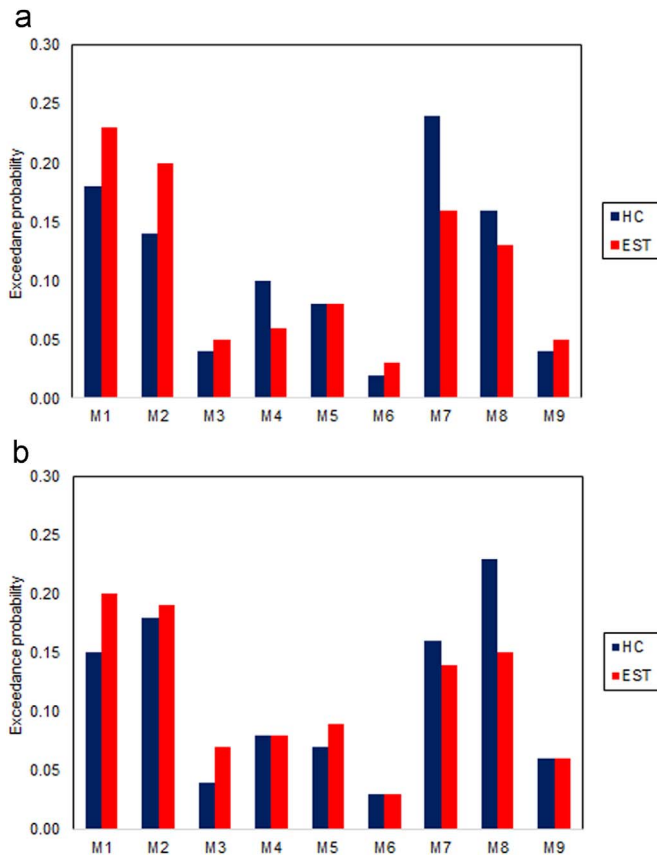[3] In this study, SZ were treated with a variety of FGA and SGA.

Fig. 3. Exceedance probabilities for bilinear models in both hemispheres (A) Exceedance probabilities for bilinear models – Left hemisphere. (B) Exceedance probabilities for bilinear models – Right hemisphere. Results for HC are based on model 7 and results for EST are based on model 1 (Fig. 1A). EST, patients with established schizophrenia; HC, healthy controls; M1, model 1; M7, model; *Xp,* Exceedance probability.

Fig. 4. Bayesian Model Selection results at the model family level in both hemispheres. (A) Bayesian Model Selection results at the model family level – Left hemisphere. (B) Bayesian Model Selection results at the model family level – Right hemisphere. Results for HC are based on Model 7 and results for EST are based on Model 1 (Fig. 1A). EST, patients with established schizophrenia; HC, healthy controls; *Xp,* Exceedance probability. MF1, model family 1, bilinear model. MF2, model family 2, nonlinear models – DLPFC. MF3, model family 3, nonlinear models – VTA/SN.

the right MFG to the right SPL in ARMS in contrast to HC as evaluated by BMA after *different* optimal large-scale networks were found (Schmidt et al., 2014). In these studies BMA was used to average the weights of the entire model space under the assumption that the same winning model is used by all groups to enable statistical group analyses. Those group differences in task-dependent EC are findings in their own right under the widely shared notion of the *same* functional network utilization among groups.

The findings of nonlinear connection strengths of the meso-cortical and cortico-mesal connection in working memory in SZ and HC have not been reported previously to our knowledge. We were not able to confirm our hypothesis of *different* connection strengths with nonlinear modulation of the bidirectional connection between the DLPFC and VTA/SN area between SZ and HC. This was due to the result of *different* functional bilinear networks following the heuristic search protocol (Dauvermann et al., 2013). According to the conditions of the heuristic search protocol, connection strengths with nonlinear modulation can only be statistically compared between groups if both groups display the *same* optimal bilinear networks. 'We consider that the similar likelihoods of the two most likely model families in HC may indicate that the successful performance of working memory function is dependent on the balance of nonlinear modulations of *both* the meso-cortical and the cortico-mesal connection rather than only one of the connections.' Nonetheless, these findings offer novel insight into neurobiological pathways that may underlie neuronal responses in schizophrenia. In future studies, it needs to be investigated whether the *differently* lateralized findings indicate a *dysfunctional* network system (given the altered BOLD responses) or an *alternative functional network* in SZ (given the comparable behavioral performance).
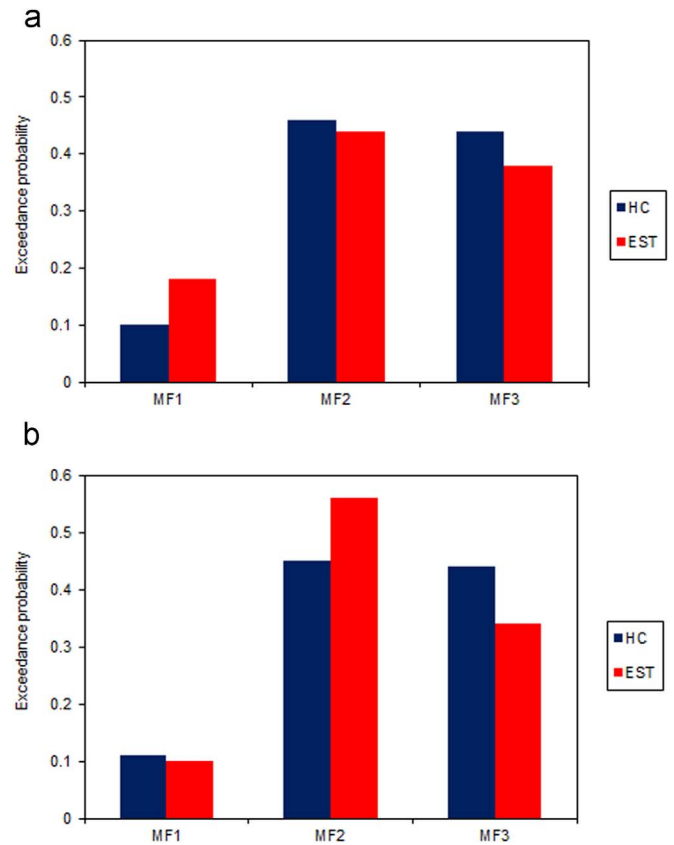
Support for the functional role of the VTA/midbrain and the implication of dopaminergic alterations in verbal/numeric working memory involving the DLPFC in SZ in contrast to HC comes from PET studies (Abi-Dargham et al., 2002; Carter et al., 1998; Fusar-Poli et al., 2010; Meyer-Lindenberg et al., 2001, 2005b). Furthermore, findings of an interaction between midbrain dopamine synthesis capacity and prefrontal function of working memory have been presented. Reduced dopamine synthesis in the midbrain was related to decreased regional cerebral blood flow of the DLPFC during working memory in HC (Meyer-Lindenberg et al., 2005a). In addition, performance of the continuous performance test in HC was associated with relatively higher magnitude of net blood brain clearance of [18F] fluorodopamine in the midbrain (Vernaleken et al., 2007). Lastly, [18F] fluorodopamine turnover in the midbrain has been shown to be increased in unmedicated SZ compared to HC (Kumakura et al., 2007).

Currently, it is not understood what the neurocognitive and neuropsychological processes of gating or their effects in working memory in humans are. However, we suggest that intact gating may lead to successful performance of working memory given the comparable performance levels in this study and based on electroencephalogram studies which have previously reported on the relevance of intact sensory gating during working memory tasks (Huang et al., 2013; Lijffijt et al., 2009; Shimi and Astle, 2013).

The limitations of the DCM8 approach have been discussed previously (Daunizeau et al., 2011a, 2011b). The networks in this study were limited to intra-hemispheric networks, whereas it can be assumed that working memory is also processed inter-hemispherically (Wheeler et al., 2014). The systematic testing of EC measures on task-dependent
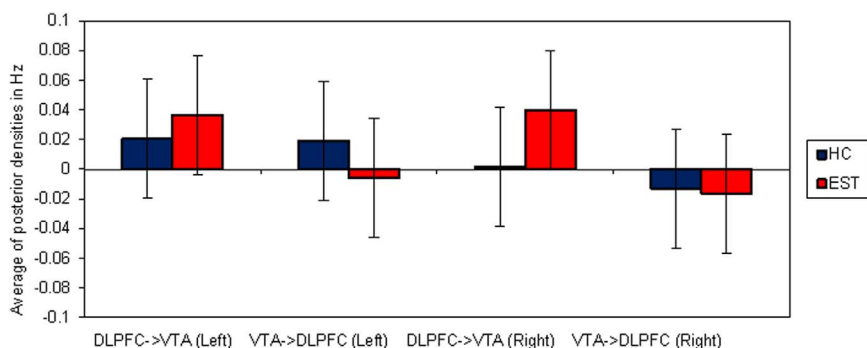
Fig. 5. Average of posterior densities of connection strength with nonlinear modulation in both hemispheres. Results for HC are based on Model 7_DLPFC_VTA/SN_DLPFC and results for EST are based on Model 1_DLPFC_VTA/SN_DLPFC (Fig. 2). DLPFC- > VTA (left), connection from DLPFC to VTA/SN area – left hemisphere; cortico-mesal connection; EST, patients with schizophrenia; HC, healthy controls; Hz, Hertz.

modulation can only be considered for the specific experimental task and the given model space for the bilinear and nonlinear models. Therefore, it has to be acknowledged that EC measures between brain regions for any examined model space may be different among individuals, including the task modulation from the IPS to the DLPFC. We acknowledge a caveat that antipsychotic medication may have affected our EC findings in addition to the lack of dopamine concentration measurement in the midbrain in this study. However it has been established that glutamatergic and dopaminergic alterations in the PFC (Coyle, 2006; Kantrowitz and Javitt, 2010; Laruelle, 2014), midbrain (Abi-Dargham et al., 2002; Durstewitz and Seamans, 2002) and their interactions within the PFC – midbrain circuit (Gao and Wolf, 2007, 2008) underlie working memory in schizophrenia (Arnsten et al., 2012; Goldman-Rakic and Selemon, 1997; Lewis and Moghaddam, 2006; Moghaddam et al., 1997; Tanaka, 2006; Timofeeva and Levin, 2011). Furthermore, glutamatergic concentrations from prefrontal brain regions in SZ when compared to HC as measured with Proton Magnetic Resonance Spectroscopy (MRS) are missing in this article. However, recent MRS, proton echo planar spectroscopic imaging and multi-modal MRS and fMRI studies presented evidence for a role of prefrontal glutamatergic concentrations in the pathophysiology of schizophrenia (Poels et al., 2014; Xu et al., 2016) and higher cognitive performance in SZ and/or HC (Bustillo et al., 2011; Ohrmann et al., 2008, 2007; Shirayama et al., 2010), including working memory (Chen et al., 2014; Michels et al., 2012). We cannot exclude the possibility of other illness or medication effects. Lastly, it is acknowledged that the sample size for the two groups was small but comparable to other published DCM studies in schizophrenia (Dima et al., 2009; Allen et al., 2010; Bastos-Leite et al., 2015).[4]

Taken together, the findings suggest that the analysis of functional large-scale networks may lead to a better understanding of cortical connectivity and glutamatergic alterations in working memory in patients with schizophrenia.

Contributions

The following authors contributed to these parts of the work: Study design (MD, TM, LR, JH, NR, ZH, NB, DB, AM, SL), acquisition of data (MD, TM, AW, BD, LR, DB), analysis of the data (MD, TM, AW, BD, GL), interpretation of the work (MD, TM, GL, SL), writing the manuscript (MD, TM, GL) or revising the manuscript (MD, TM, JH, NR, GL, ZH, NB, BW, DB, AM, SL), final approval of the work (MD, TM, AW, BD, LR, JH, NR, GL, ZH, NB, BW, DB, AM, SL), and agreement to be accountable for the work (MD, TM, AW, BD, LR, JH, NR, GL, ZH, NB, BW, DB, AM, SL).

Conflicts of interests

MD and TM were supported by Dr. Mortimer and Theresa Sackler Foundation throughout the project. No conflicts of interest are declared.

TM, AW and BD received funding from Pfizer through the study. No conflicts of interest are declared.

ZH and is a current full time employee of Pfizer Inc.

NB is a former full time employees of Pfizer Inc.; NB is current full time employees of AstraZeneca Plc.

SL has received personal fees from Janssen, Roche and Sunovion, and research grants from Abbvie, Roche and Pfizer. LR, JH, NR, GL, DB, AMcI report no conflicts of interest.

The following affiliations were directly involved in the study

Division of Psychiatry, University of Edinburgh, Edinburgh, UK
Clinical Research Imaging Centre, University of Edinburgh, Edinburgh, UK
Neuroscience Research Unit, Pfizer Inc, Cambridge, MA, USA
Clinical and Translational Imaging, Pfizer Inc., Cambridge, MA, USA

These are current affiliations

School of Psychology, National University of Ireland Galway, University Road, Galway, Ireland
McGovern Institute for Brain Research, Massachusetts Institute of Technology, Boston, USA
Neuroscience and Mental Health Research Institute, Cardiff

---

[4] We note that it is conceivable that *different* networks may include the following alternative interpretations: (i) Both groups are using the *same* networks but (at least) one group utilizes (at least) one additional network that differs from the first network; (ii) *Different* networks are defined by different brain regions, different number of brain regions, different connections and/or modulations. In this study, we cannot test these alternative hypotheses.

University, Cardiff, UK

British Heart Foundation Centre for Cardiovascular Science, University of Edinburgh, Edinburgh, UK

AstraZeneca, IMED Neuroscience Unit, Waltham, MA, USA

References

Abbott, L.F., Varela, J.A., Sen, K., Nelson, S.B., 1997. Synaptic depression and cortical gain control. Science 275, 220–224.

Abi-Dargham, A., Mawlawi, O., Lombardo, I., Gil, R., Martinez, D., Huang, Y., Hwang, D.R., Keilp, J., Kochan, L., Van Heertum, R., Gorman, J.M., Laruelle, M., 2002. Prefrontal dopamine D1 receptors and working memory in schizophrenia. J. Neurosci.: Off. J. Soc. Neurosci. 22, 3708–3719.

Allen, P., Stephan, K.E., Mechelli, A., Day, F., Ward, N., Dalton, J., Williams, S.C., McGuire, P., 2010. Cingulate activity and fronto-temporal connectivity in people with prodromal signs of psychosis. Neuroimage 49 (1), 947–955.

Andreasen, N.C., 1989. The Scale for the Assessment of Negative Symptoms (SANS): conceptual and theoretical foundations. Br. J. Psychiatry Suppl. 49–58.

Arnsten, A.F., Paspalas, C.D., Gamo, N.J., Yang, Y., Wang, M., 2010. Dynamic Network Connectivity: a new form of neuroplasticity. Trends Cogn. Sci. 14, 365–375.

Arnsten, A.F., Wang, M.J., Paspalas, C.D., 2012. Neuromodulation of thought: flexibilities and vulnerabilities in prefrontal cortical network synapses. Neuron 76, 223–239.

Au-Young, S.M., Shen, H., Yang, C.R., 1999. Medial prefrontal cortical output neurons to the ventral tegmental area (VTA) and their responses to burst-patterned stimulation of the VTA: neuroanatomical and in vivo electrophysiological analyses. Synapse 34, 245–255.

Bastos-Leite, A.J., Ridgway, G.R., Silveira, C., Norton, A., Reis, S., Friston, K.J., 2015. Dysconnectivity within the default mode in first-episode schizophrenia: a stochastic dynamic causal modeling study with functional magnetic resonance imaging. Schizophr. Bull. 41 (1) 155-153.

Berends, M., Maex, R., De Schutter, E., 2005. The effect of NMDA receptors on gain modulation. Neural Comput. 17, 2531–2547.

Birnbaum, R., Weinberger, D.R., 2013. Functional neuroimaging and schizophrenia: a view towards effective connectivity modeling and polygenic risk. Dialog-. Clin. Neurosci. 15, 279–289.

Bozikas, V.P., Andreou, C., 2011. Longitudinal studies of cognition in first episode psychosis: a systematic review of the literature. Aust. N. Z. J. Psychiatry 45, 93–108.

Braver, T.S., Barch, D.M., Cohen, J.D., 1999. Cognition and control in schizophrenia: a computational model of dopamine and prefrontal function. Biol. Psychiatry 46, 312–328.

Braver, T.S., Cohen, J.D., 1999. Dopamine, cognitive control, and schizophrenia: the gating model. Prog. Brain Res. 121, 327–349.

Brazdil, M., Mikl, M., Marecek, R., Krupa, P., Rektor, I., 2007. Effective connectivity in target stimulus processing: a dynamic causal modeling study of visual oddball task. NeuroImage 35, 827–835.

Broome, M.R., Matthiasson, P., Fusar-Poli, P., Woolley, J.B., Johns, L.C., Tabraham, P., Bramon, E., Valmaggia, L., Williams, S.C., Brammer, M.J., Chitnis, X., McGuire, P.K., 2009. Neural correlates of executive function and working memory in the 'at-risk mental state'. Br. J. Psychiatry 194, 25–33.

Bustillo, J.R., Chen, H., Gasparovic, C., Mullins, P., Caprihan, A., Qualls, C., Apfeldorf, W., Lauriello, J., Posse, S., 2011. Glutamate as a marker of cognitive function in schizophrenia: a proton spectroscopic imaging study at 4 T. Biol. Psychiatry 69, 19–27.

Callicott, J.H., Bertolino, A., Mattay, V.S., Langheim, F.J., Duyn, J., Coppola, R., Goldberg, T.E., Weinberger, D.R., 2000. Physiological dysfunction of the dorsolateral prefrontal cortex in schizophrenia revisited. Cereb. Cortex 10, 1078–1092.

Callicott, J.H., Mattay, V.S., Verchinski, B.A., Marenco, S., Egan, M.F., Weinberger, D.R., 2003. Complexity of prefrontal cortical dysfunction in schizophrenia: more than up or down. Am. J. Psychiatry 160, 2209–2215.

Carter, C.S., Perlstein, W., Ganguli, R., Brar, J., Mintun, M., Cohen, J.D., 1998. Functional hypofrontality and working memory dysfunction in schizophrenia. Am. J. Psychiatry 155, 1285–1287.

Chen, C.M., Stanford, A.D., Mao, X., Abi-Dargham, A., Shungu, D.C., Lisanby, S.H., Schroeder, C.E., Kegeles, L.S., 2014. GABA level, gamma oscillation, and working memory performance in schizophrenia. NeuroImage Clin. 4, 531–539.

Constantinidis, C., Klingberg, T., 2016. The neuroscience of working memory capacity and training. Nat. Rev. Neurosci. 17, 438–449.

Coyle, J.T., 2006. Glutamate and schizophrenia: beyond the dopamine hypothesis. Cell Mol. Neurobiol. 26, 365–384.

D'Aiuto, L., Prasad, K.M., Upton, C.H., Viggiano, L., Milosevic, J., Raimondi, G., McClain, L., Chowdari, K., Tischfield, J., Sheldon, M., Moore, J.C., Yolken, R.H., Kinchington, P.R., Nimgaonkar, V.L., 2015. Persistent infection by HSV-1 is associated with changes in functional architecture of iPSC-derived neurons and brain activation patterns underlying working memory performance. Schizophr. Bull. 41, 123–132.

D'Ardenne, K., Eshel, N., Luka, J., Lenartowicz, A., Nystrom, L.E., Cohen, J.D., 2012. Role of prefrontal cortex and the midbrain dopamine system in working memory updating. Proc. Natl. Acad. Sci. USA 109, 19900–19909.

Daunizeau, J., David, O., Stephan, K.E., 2011a. Dynamic causal modelling: a critical review of the biophysical and statistical foundations. NeuroImage 58, 312–322.

Daunizeau, J., Preuschoff, K., Friston, K., Stephan, K., 2011b. Optimizing experimental design for comparing models of brain function. PLoS Comput. Biol. 7, e1002280.

Dauvermann, M.R., Whalley, H.C., Romaniuk, L., Valton, V., Owens, D.G., Johnstone, E.C., Lawrie, S.M., Moorhead, T.W., 2013. The application of nonlinear Dynamic Causal Modelling for fMRI in subjects at high genetic risk of schizophrenia. NeuroImage 73, 16–29.

Dauvermann, M.R., Whalley, H.C., Schmidt, A., Lee, G.L., Romaniuk, L., Roberts, N., Johnstone, E.C., Lawrie, S.M., Moorhead, T.W., 2014. Computational neuropsychiatry - schizophrenia as a cognitive brain network disorder. Front Psychiatry 5, 30.

Dauvermann, M.R., Lee, G., Dawson, N., 2017. Glutamatergic regulation of cognition and functional brain connectivity: insights from pharmacological, genetic and translational schizophrenia research. Br. J. Pharmacol. http://dx.doi.org/10.1111/bph.13919.

Deserno, L., Sterzer, P., Wustenberg, T., Heinz, A., Schlagenhauf, F., 2012. Reduced prefrontal-parietal effective connectivity and working memory deficits in schizophrenia. J. Neurosci.: Off. J. Soc. Neurosci. 32, 12–20.

Dima, D., Roiser, J.P., Dietrich, D.E., Bonnemann, C., Lanfermann, H., Emrich, H.M., Dillo, W., 2009. Understanding why patients with schizophrenia do not perceive the hollow-mask illusion using dynamic causal modelling. Neuroimage 46 (4), 1180–1186.

Durstewitz, D., Seamans, J.K., 2002. The computational role of dopamine D1 receptors in working memory. Neural Netw. 15, 561–572.

Durstewitz, D., Seamans, J.K., 2008. The dual-state theory of prefrontal cortex dopamine function with relevance to catechol-o-methyltransferase genotypes and schizophrenia. Biol. Psychiatry 64, 739–749.

Eryilmaz, H., Tanner, A.S., Ho, N.F., Nitenson, A.Z., Silverstein, N.J., Petruzzi, L.J., Goff, D.C., Manoach, D.S., Roffman, J.L., 2016. Disrupted working memory circuitry in schizophrenia: disentangling fMRI markers of core pathology vs other aspects of impaired performance. Neuropsychopharmacol.: Off. Publ. Am. Coll. Neuropsychopharmacol. 41, 2411–2420.

First, M.B., Spitzer, Robert, L., Miriam, Gibbon, Williams, Janet, B.W., 2002. (SCID-I/P). Structured Clinical Interview for DSM-IV-TR Axis I Disorders, Research Version, Patient edition. Biometrics Research, New York.

Friston, K., Brown, H.R., Siemerkus, J., Stephan, K.E., 2016. The dysconnection hypothesis (2016). Schizophr. Res. 176, 83–94.

Friston, K.J., Dolan, R.J., 2010. Computational and dynamic models in neuroimaging. NeuroImage 52, 752–765.

Friston, K.J., Frith, C.D., 1995. Schizophrenia: a disconnection syndrome? Clin. Neurosci. 3, 89–97.

Friston, K.J., Harrison, L., Penny, W., 2003. Dynamic causal modelling. NeuroImage 19, 1273–1302.

Fusar-Poli, P., Howes, O.D., Allen, P., Broome, M., Valli, I., Asselin, M.C., Grasby, P.M., McGuire, P.K., 2010. Abnormal frontostriatal interactions in people with prodromal signs of psychosis: a multimodal imaging study. Arch. Gen. Psychiatry 67, 683–691.

Gao, C., Wolf, M.E., 2007. Dopamine alters AMPA receptor synaptic expression and subunit composition in dopamine neurons of the ventral tegmental area cultured with prefrontal cortex neurons. J. Neurosci.: Off. J. Soc. Neurosci. 27, 14275–14285.

Gao, C., Wolf, M.E., 2008. Dopamine receptors regulate NMDA receptor surface expression in prefrontal cortex neurons. J. Neurochem. 106, 2489–2501.

Gao, W.J., Wang, Y., Goldman-Rakic, P.S., 2003. Dopamine modulation of perisomatic and peridendritic inhibition in prefrontal cortex. J. Neurosci.: Off. J. Soc. Neurosci. 23, 1622–1630.

Genevsky, A., Garrett, C.T., Alexander, P.P., Vinogradov, S., 2010. Cognitive training in schizophrenia: a neuroscience-based approach. Dialog-. Clin. Neurosci. 12, 416–421.

Genovese, C.R., Lazar, N.A., Nichols, T., 2002. Thresholding of statistical maps in functional neuroimaging using the false discovery rate. NeuroImage 15, 870–878.

Girault, J.A., Greengard, P., 2004. The neurobiology of dopamine signaling. Arch. Neurol. 61, 641–644.

Glahn, D.C., Ragland, J.D., Abramoff, A., Barrett, J., Laird, A.R., Bearden, C.E., Velligan, D.I., 2005. Beyond hypofrontality: a quantitative meta-analysis of functional neuroimaging studies of working memory in schizophrenia. Hum. Brain Mapp. 25, 60–69.

Gold, J.M., 2004. Cognitive deficits as treatment targets in schizophrenia. Schizophr. Res. 72, 21–28.

Goldman-Rakic, P.S., Selemon, L.D., 1997. Functional and anatomical aspects of prefrontal pathology in schizophrenia. Schizophr. Bull. 23, 437–458.

Guerrero-Pedraza, A., McKenna, P.J., Gomar, J.J., Sarro, S., Salvador, R., Amann, B., Carrion, M.I., Landin-Romero, R., Blanch, J., Pomarol-Clotet, E., 2012. First-episode psychosis is characterized by failure of deactivation but not by hypo- or hyperfrontality. Psychol. Med. 42, 73–84.

Huang, L.Y., She, H.C., Chou, W.C., Chuang, M.H., Duann, J.R., Jung, T.P., 2013. Brain oscillation and connectivity during a chemistry visual working memory task. Int. J. Psychophysiol.: Off. J. Int. Organ. Psychophysiol. 90, 172–179.

Javitt, D.C., 2007. Glutamate and schizophrenia: phencyclidine, N-methyl-D-aspartate receptors, and dopamine-glutamate interactions. Int Rev. Neurobiol. 78, 69–108.

Kantrowitz, J.T., Javitt, D.C., 2010. Thinking glutamatergically: changing concepts of schizophrenia based upon changing neurochemical models. Clin. Schizophr. Relat. Psychoses 4, 189–200.

Kay, S.R., Fiszbein, A., Opler, L.A., 1987. The positive and negative syndrome scale (PANSS) for schizophrenia. Schizophr. Bull. 13, 261–276.

Kumakura, Y., Cumming, P., Vernaleken, I., Buchholz, H.G., Siessmeier, T., Heinz, A., Kienast, T., Bartenstein, P., Grunder, G., 2007. Elevated [18F]fluorodopamine turnover in brain of patients with schizophrenia: an [18F]fluorodopa/positron emission tomography study. J. Neurosci.: Off. J. Soc. Neurosci. 27, 8080–8087.

Laruelle, M., 2014. Schizophrenia: from dopaminergic to glutamatergic interventions. Curr. Opin. Pharmacol. 14, 97–102.

Laruelle, M., Frankle, W.G., Narendran, R., Kegeles, L.S., Abi-Dargham, A., 2005. Mechanism of action of antipsychotic drugs: from dopamine D(2) receptor antagonism to glutamate NMDA facilitation. Clin. Ther. 27 (Suppl A), S16–S24.

Lewis, D.A., Moghaddam, B., 2006. Cognitive dysfunction in schizophrenia: convergence of gamma-aminobutyric acid and glutamate alterations. Arch. Neurol. 63,

1372–1376.

Lijffijt, M., Lane, S.D., Meier, S.L., Boutros, N.N., Burroughs, S., Steinberg, J.L., Moeller, F.G., Swann, A.C., 2009. P50, N100, and P200 sensory gating: relationships with behavioral inhibition, attention, and working memory. Psychophysiology 46, 1059–1068.

Macmillan, N.A., Creelman, C.D., 1991. Detection Theory: A User's Guide. Cambridge University, Cambridge.

Macmillan, N.A., Kaplan, H.L., 1985. Detection theory analysis of group data: estimating sensitivity from average hit and false-alarm rates. Psychol. Bull. 98, 185–199.

Meyer-Lindenberg, A., Kohn, P.D., Kolachana, B., Kippenhan, S., McInerney-Leo, A., Nussbaum, R., Weinberger, D.R., Berman, K.F., 2005a. Midbrain dopamine and prefrontal function in humans: interaction and modulation by COMT genotype. Nat. Neurosci. 8, 594–596.

Meyer-Lindenberg, A., Poline, J.B., Kohn, P.D., Holt, J.L., Egan, M.F., Weinberger, D.R., Berman, K.F., 2001. Evidence for abnormal cortical functional connectivity during working memory in schizophrenia. Am. J. Psychiatry 158, 1809–1817.

Meyer-Lindenberg, A.S., Olsen, R.K., Kohn, P.D., Brown, T., Egan, M.F., Weinberger, D.R., Berman, K.F., 2005b. Regionally specific disturbance of dorsolateral prefrontal-hippocampal functional connectivity in schizophrenia. Arch. Gen. Psychiatry 62, 379–386.

Michels, L., Martin, E., Klaver, P., Edden, R., Zelaya, F., Lythgoe, D.J., Luchinger, R., Brandeis, D., O'Gorman, R.L., 2012. Frontal GABA levels change during working memory. PLoS One 7, e31933.

Moghaddam, B., Adams, B., Verma, A., Daly, D., 1997. Activation of glutamatergic neurotransmission by ketamine: a novel step in the pathway from NMDA receptor blockade to dopaminergic and cognitive disruptions associated with the prefrontal cortex. J. Neurosci.: Off. J. Soc. Neurosci. 17, 2921–2927.

Murphy, B.K., Miller, K.D., 2003. Multiplicative gain changes are induced by excitation or inhibition alone. J. Neurosci.: Off. J. Soc. Neurosci. 23, 10040–10051.

Murty, V.P., Sambataro, F., Radulescu, E., Altamura, M., Iudicello, J., Zoltick, B., Weinberger, D.R., Goldberg, T.E., Mattay, V.S., 2011. Selective updating of working memory content modulates meso-cortico-striatal activity. NeuroImage 57, 1264–1272.

Neher, E., Sakaba, T., 2008. Multiple roles of calcium ions in the regulation of neurotransmitter release. Neuron 59, 861–872.

Ohrmann, P., Kugel, H., Bauer, J., Siegmund, A., Kolkebeck, K., Suslow, T., Wiedl, K.H., Rothermundt, M., Arolt, V., Pedersen, A., 2008. Learning potential on the WCST in schizophrenia is related to the neuronal integrity of the anterior cingulate cortex as measured by proton magnetic resonance spectroscopy. Schizophr. Res. 106, 156–163.

Ohrmann, P., Siegmund, A., Suslow, T., Pedersen, A., Spitzberg, K., Kersting, A., Rothermundt, M., Arolt, V., Heindel, W., Pfleiderer, B., 2007. Cognitive impairment and in vivo metabolites in first-episode neuroleptic-naive and chronic medicated schizophrenic patients: a proton magnetic resonance spectroscopy study. J. Psychiatr. Res. 41, 625–634.

Onn, S.P., Wang, X.B., 2005. Differential modulation of anterior cingulate cortical activity by afferents from ventral tegmental area and mediodorsal thalamus. Eur. J. Neurosci. 21, 2975–2992.

Owen, A.M., McMillan, K.M., Laird, A.R., Bullmore, E., 2005. N-back working memory paradigm: a meta-analysis of normative functional neuroimaging studies. Hum. Brain Mapp. 25, 46–59.

Pan, B., Zucker, R.S., 2009. A general model of synaptic transmission and short-term plasticity. Neuron 62, 539–554.

Pedersen, G., Karterud, S., 2012. The symptom and function dimensions of the Global Assessment of Functioning (GAF) scale. Compr. Psychiatry 53, 292–298.

Penny, W.D., Stephan, K.E., Daunizeau, J., Rosa, M.J., Friston, K.J., Schofield, T.M., Leff, A.P., 2010. Comparing families of dynamic causal models. PLoS Comput. Biol. 6, e1000709.

Penny, W.D., Stephan, K.E., Mechelli, A., Friston, K.J., 2004. Comparing dynamic causal models. Neuroimage 22, 1157–1172.

Perlstein, W.M., Carter, C.S., Noll, D.C., Cohen, J.D., 2001. Relation of prefrontal cortex dysfunction to working memory and symptoms in schizophrenia. Am. J. Psychiatry 158, 1105–1113.

Poels, E.M., Kegeles, L.S., Kantrowitz, J.T., Javitt, D.C., Lieberman, J.A., Abi-Dargham, A., Girgis, R.R., 2014. Glutamatergic abnormalities in schizophrenia: a review of proton MRS findings. Schizophr. Res. 152, 325–332.

Quide, Y., Morris, R.W., Shepherd, A.M., Rowland, J.E., Green, M.J., 2013. Task-related fronto-striatal functional connectivity during working memory performance in schizophrenia. Schizophr. Res. 150, 468–475.

Rasetti, R., Sambataro, F., Chen, Q., Callicott, J.H., Mattay, V.S., Weinberger, D.R., 2011. Altered cortical network dynamics: a potential intermediate phenotype for schizophrenia and association with ZNF804A. Arch. Gen. Psychiatry 68, 1207–1217.

Rothman, J.S., Cathala, L., Steuber, V., Silver, R.A., 2009. Synaptic depression enables neuronal gain control. Nature 457, 1015–1018.

Salinas, E., Sejnowski, T.J., 2000. Impact of correlated synaptic input on output firing rate and variability in simple neuronal models. J. Neurosci.: Off. J. Soc. Neurosci. 20, 6193–6209.

Salinas, E., Sejnowski, T.J., 2001. Gain modulation in the central nervous system: where behavior, neurophysiology, and computation meet. Neuroscientist 7, 430–440.

Schlosser, R., Gesierich, T., Kaufmann, B., Vucurevic, G., Hunsche, S., Gawehn, J., Stoeter, P., 2003a. Altered effective connectivity during working memory performance in schizophrenia: a study with fMRI and structural equation modeling. NeuroImage 19, 751–763.

Schlosser, R., Gesierich, T., Kaufmann, B., Vucurevic, G., Stoeter, P., 2003b. Altered effective connectivity in drug free schizophrenic patients. Neuroreport 14, 2233–2237.

Schlosser, R.G., Koch, K., Wagner, G., Nenadic, I., Roebel, M., Schachtzabel, C., Axer, M., Schultz, C., Reichenbach, J.R., Sauer, H., 2008. Inefficient executive cognitive control

in schizophrenia is preceded by altered functional activation during information encoding: an fMRI study. Neuropsychologia 46, 336–347.

Schlosser, R.G., Wagner, G., Sauer, H., 2006. Assessing the working memory network: studies with functional magnetic resonance imaging and structural equation modeling. Neuroscience 139, 91–103.

Schmidt, A., Smieskova, R., Aston, J., Simon, A., Allen, P., Fusar-Poli, P., McGuire, P.K., Riecher-Rossler, A., Stephan, K.E., Borgwardt, S., 2013. Brain connectivity abnormalities predating the onset of psychosis: correlation with the effect of medication. JAMA Psychiatry 70, 903–912.

Schmidt, A., Smieskova, R., Simon, A., Allen, P., Fusar-Poli, P., McGuire, P.K., Bendfeldt, K., Aston, J., Lang, U.E., Walter, M., Radue, E.W., Riecher-Rossler, A., Borgwardt, S.J., 2014. Abnormal effective connectivity and psychopathological symptoms in the psychosis high-risk state. J. Psychiatry Neurosci.: JPN 39, 239–248.

Shimi, A., Astle, D.E., 2013. The strength of attentional biases reduces as visual short-term memory load increases. J. Neurophysiol. 110, 12–18.

Shirayama, Y., Obata, T., Matsuzawa, D., Nonaka, H., Kanazawa, Y., Yoshitome, E., Ikehira, H., Hashimoto, K., Iyo, M., 2010. Specific metabolites in the medial prefrontal cortex are associated with the neurocognitive deficits in schizophrenia: a preliminary study. NeuroImage 49, 2783–2790.

Stephan, K.E., Baldeweg, T., Friston, K.J., 2006. Synaptic plasticity and dysconnection in schizophrenia. Biol. Psychiatry 59, 929–939.

Stephan, K.E., Friston, K.J., Frith, C.D., 2009. Dysconnection in schizophrenia: from abnormal synaptic plasticity to failures of self-monitoring. Schizophr. Bull. 35, 509–527.

Stephan, K.E., Harrison, L.M., Kiebel, S.J., David, O., Penny, W.D., Friston, K.J., 2007. Dynamic causal models of neural system dynamics: current state and future extensions. J. Biosci. 32, 129–144.

Stephan, K.E., Kasper, L., Harrison, L.M., Daunizeau, J., den Ouden, H.E., Breakspear, M., Friston, K.J., 2008. Nonlinear dynamic causal models for fMRI. NeuroImage 42, 649–662.

Sun, Y.G., Beierlein, M., 2011. Receptor saturation controls short-term synaptic plasticity at corticothalamic synapses. J. Neurophysiol. 105, 2319–2329.

Takahata, R., Moghaddam, B., 1998. Glutamatergic regulation of basal and stimulus-activated dopamine release in the prefrontal cortex. J. Neurochem. 71, 1443–1449.

Tan, H.Y., Sust, S., Buckholtz, J.W., Mattay, V.S., Meyer-Lindenberg, A., Egan, M.F., Weinberger, D.R., Callicott, J.H., 2006. Dysfunctional prefrontal regional specialization and compensation in schizophrenia. Am. J. Psychiatry 163, 1969–1977.

Tanaka, S., 2006. Dopaminergic control of working memory and its relevance to schizophrenia: a circuit dynamics perspective. Neuroscience 139, 153–171.

Thermenos, H.W., Goldstein, J.M., Buka, S.L., Poldrack, R.A., Koch, J.K., Tsuang, M.T., Seidman, L.J., 2005. The effect of working memory performance on functional MRI in schizophrenia. Schizophr. Res. 74, 179–194.

Timofeeva, O.A., Levin, E.D., 2011. Glutamate and nicotinic receptor interactions in working memory: importance for the cognitive impairment of schizophrenia. Neuroscience 195, 21–36.

Tseng, K.Y., O'Donnell, P., 2004. Dopamine-glutamate interactions controlling prefrontal cortical pyramidal cell excitability involve multiple signaling mechanisms. J. Neurosci.: Off. J. Soc. Neurosci. 24, 5131–5139.

Tzschentke, T.M., 2001. Pharmacology and behavioral pharmacology of the mesocortical dopamine system. Prog. Neurobiol. 63, 241–320.

Vernaleken, I., Buchholz, H.G., Kumakura, Y., Siessmeier, T., Stoeter, P., Bartenstein, P., Cumming, P., Grunder, G., 2007. 'Prefrontal' cognitive performance of healthy subjects positively correlates with cerebral FDOPA influx: an exploratory [18F]-fluoro-L-DOPA-PET investigation. Hum. Brain Mapp. 28, 931–939.

Volman, V., Levine, H., Sejnowski, T.J., 2010. Shunting inhibition controls the gain modulation mediated by asynchronous neurotransmitter release in early development. PLoS Comput. Biol. 6, e1000909.

Wang, L., Liu, X., Guise, K.G., Knight, R.T., Ghajar, J., Fan, J., 2010. Effective connectivity of the fronto-parietal network during attentional control. J. Cogn. Neurosci. 22, 543–553.

Wang, X.J., 2010. Neurophysiological and computational principles of cortical rhythms in cognition. Physiol. Rev. 90, 1195–1268.

Weinberger, D.R., 1993. A connectionist approach to the prefrontal cortex. J. Neuropsychiatry Clin. Neurosci. 5, 241–253.

Wheeler, A.L., Chakravarty, M.M., Lerch, J.P., Pipitone, J., Daskalakis, Z.J., Rajji, T.K., Mulsant, B.H., Voineskos, A.N., 2014. Disrupted prefrontal interhemispheric structural coupling in schizophrenia related to working memory performance. Schizophr. Bull. 40, 914–924.

Xu, H., Zhang, H., Zhang, J., Huang, Q., Shen, Z., Wu, R., 2016. Evaluation of neuron-glia integrity by in vivo proton magnetic resonance spectroscopy: implications for psychiatric disorders. Neurosci. Biobehav. Rev. 71, 563–577.

Xu, J., Zhang, S., Calhoun, V.D., Monterosso, J., Li, C.S., Worhunsky, P.D., Stevens, M., Pearlson, G.D., Potenza, M.N., 2013. Task-related concurrent but opposite modulations of overlapping functional networks as revealed by spatial ICA. NeuroImage 79, 62–71.

Yahata, N., Kasai, K., Kawato, M., 2017. Computational neuroscience approach to biomarkers and treatments for mental disorder. Psychiatry Clin. Neurosci. 71 (4), 215–237.

Yu, Y., FitzGerald, T.H., Friston, K.J., 2013. Working memory and anticipatory set modulate midbrain and putamen activity. J. Neurosci.: Off. J. Soc. Neurosci. 33, 14040–14047.

Zhang, H., Wei, X., Tao, H., Mwansisya, T.E., Pu, W., He, Z., Hu, A., Xu, L., Liu, Z., Shan, B., Xue, Z., 2013. Opposite effective connectivity in the posterior cingulate and medial prefrontal cortex between first-episode schizophrenic patients with suicide risk and healthy controls. PLloS One 8, e63477.